JOC The Journal of Organic Chemistry

ARTICLE

pubs.acs.org/joc

Effects of Chemical Structure on the Thermodynamic Efficiency of Radical Chain Carriers for Organic Synthesis

Ching Yeh Lin, Jessie Peh,† and Michelle L. Coote*

ARC Centre of Excellence for Free-Radical Chemistry and Biotechnology, Research School of Chemistry, Australian National University, Canberra ACT 0200, Australia

Supporting Information

ABSTRACT: The chain carrier index (CCI), defined as the ratio of the bond dissociation free energies (BDFE) of corresponding chain carrier halides and hydrides, is proposed as a measure of the thermodynamic efficiency of chain carriers for radical dehalogenation. The larger this value is relative to the corresponding value of the organic substrate, the more thermodynamically efficient the process. The chloride and bromide CCIs were evaluated at the G3(MP2)-RAD(+) level of theory for 120 different R-groups, covering a broad range of carbon-centered and noncarbon-centered species; the effects of solvent and temperature have also been studied. The broad finding from this work is that successful chain carriers generally maximize the strength of their halide (versus hydride bonds) through charge-shift bonding. As a result, the thermodynamic efficiency of a chain carrier tends to increase down the periodic table, and also with the inclusion of stronger electron donating substituents. The CCIs of carbon-centered species fall into a relatively narrow range so that, even when the CCI is maximized through inclusion of lone pair donor OMe or NMe_2 groups, the thermodynamic driving force for dehalogenation of other organic substrates is modest at best, and the process is likely to be kinetically hampered. Among the noncarbon-centered species studied, bismuth- and borane-centered compounds have some of the highest CCI values and, although their kinetics requires further optimization, these classes of compounds would be worth further investigation as tin-free radical reducing agents.

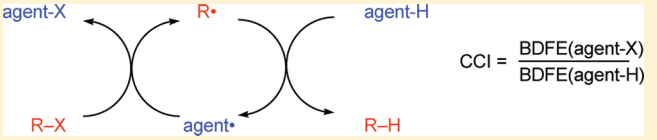

INTRODUCTION

Radical reactions have become popular among organic chemists as they can be used to achieve chemoselective transformations of predictable regio- and stereochemical outcomes with use of mild conditions.[1] In particular, the introduction of radical reducing agents has led to a rapid growth in the number of organic transformations that make use of radicals to affect dehalogenation,[2,3] often accompanied by other reactions such as ring closure.[4] In a typical radical dehalogenation reaction, such as the generic example provided in Scheme 1, free radicals are first produced via decomposition of a free radical initiator (reaction a) followed by hydrogen abstraction from a chain carrier agent such as $Sn(Bu)_3H$ (reaction b). The resulting radical chain carrier then abstracts a halogen atom from the organic substrate forming the organic substrate radical (reaction c). The organic substrate radical may then undergo chemical transformations such as ring closure (reaction d), before abstracting a hydrogen atom from another chain carrier agent forming the desired dehalogenated product and a new chain carrier radical (reaction e). This chain carrier radical can then abstract a halogen from the next molecule of organic substrate (i.e., reaction c), and the process continues until all of the reagents are converted to products, and/or the radicals are consumed in competing bimolecular termination processes (reaction f).

For a transformation to be effective, the chain carrier radical needs to be sufficiently unstable to abstract a halogen atom from the organic substrate (reaction c, Scheme 1). At the same time, it cannot be too unstable or its formation will then be disfavored when the organic product radical abstracts hydrogen from the chain carrier agent (reaction e, Scheme 1). Satisfying this delicate balancing act, while also addressing the other requirements of a good reagent (such as low toxicity, high solubility, resistance to unwanted side reactions, and low cost) is often difficult. From a thermodynamic and kinetic perspective, tributyltin hydride (Bu_3SnH) is one of the most successful mediators of free radical chain reactions. However, like other organotin compounds, it is toxic,[5] and difficult to remove completely from the desired products. In the late 1980s, tris(trimethylsilyl)silane[6] ($(TMS)_3SiH$) and subsequently in the early 1990s ethyl piperidium hypophosphite (EPHP; the chain carrier in this case is $H_2PO_2^-$)[7] were introduced as alternative reagents to tin hydride. However, $(TMS)_3SiH$ is expensive and not easy to prepare, while EPHP needs to be used in large excess with high concentrations of radical initiator. Triorganogermanes have also been investigated as tin hydride replacements and show promising characteristics but are expensive and have a high propensity to undergo side reactions with alkenes.[1] While $(TMS)_3CH$ was recently proposed as a new low-cost carbon-based agent,[8] it was subsequently found to be ineffective in mediating radical reactions.[9]

Received: November 29, 2010
Published: January 31, 2011

Scheme 1. Radical Dehalogenation Mediated by Bu_3SnH

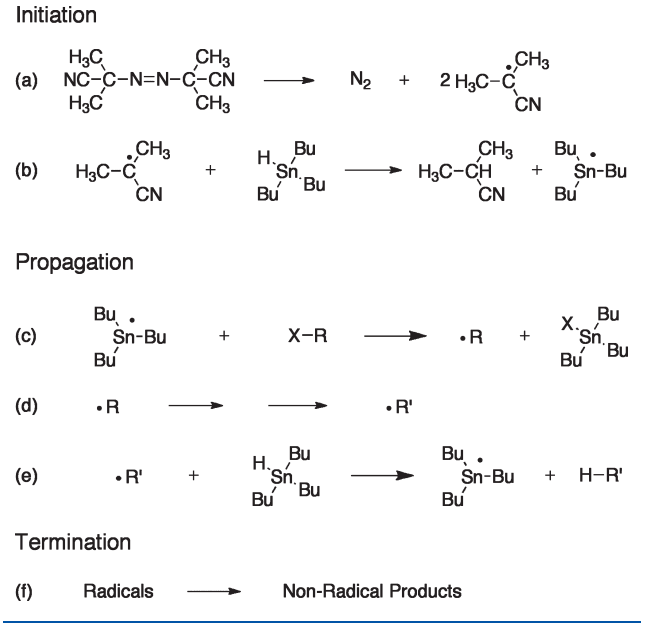

In view of the difficulties faced in choosing an appropriate radical reducing agent, it is useful to analyze why chain carriers such as Bu_3SnH or $(TMS)_3SiH$ are such effective mediators of radical reactions and ascertain whether alternative classes of compounds might offer suitable replacements for them. To this end, in the present work we use high-level ab initio molecular orbital calculations to study the effects of chemical structure and other reaction conditions on the thermodynamic efficiency of a broad range of possible radical chain carriers, and we also examine the kinetic efficiency of selected species.

THEORETICAL PROCEDURES

Thermodynamic Considerations. To maximize the thermodynamic efficiency in Scheme 1, we have to find chain carrier agents that will undergo reactions b, c, and e successfully. Because both reactions b and e are testing the ability of agents to donate hydrogen atoms, we can simplify our focus to the propagation steps c and e. In reaction c, the chain carrier radical (agent$^\bullet$) must readily abstract a halogen from the organic substrate (R−X) to form the substrate radical (R$^\bullet$) and the chain carrier halide (agent−X). The free energy change of this process depends on the relative bond dissociation free energies (BDFEs) of substrate and chain carrier *halides*.

$$\text{agent}^\bullet + \text{substrate}-\text{X} \xrightarrow{\Delta G_c} \text{agent}-\text{X} + \text{substrate}^\bullet \qquad (1)$$

$$\Delta G_c = \text{BDFE}(\text{substrate}-\text{X}) - \text{BDFE}(\text{agent}-\text{X})$$

This reaction is thermodynamically favored if the agent−X BDFE is larger than the corresponding substrate−X BDFE (i.e., the agent makes a stronger bond with the halogen than does the substrate). In reaction e, the substrate radical (or the rearranged product radical, if there is an accompanying rearrangement at d) then abstracts hydrogen from the next chain carrier agent, producing the final dehalogenated product and the next chain carrier radical that can then continue the process. For this step, the free energy changes depend on the relative BDFEs of the

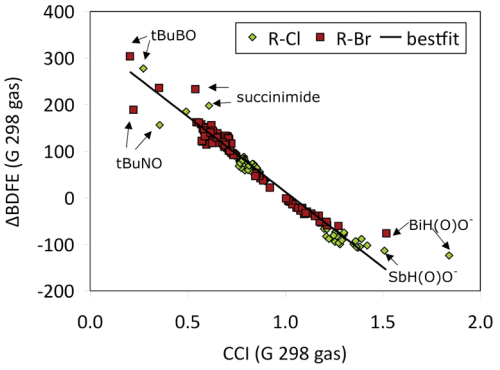

Figure 1. Comparison of the gas-phase 298.15 K ΔBDFE and CCI indices for the test set. The ΔBDFE index is defined as the difference of corresponding R−X and R−H bond dissociation free energies while the CCI is defined as their ratio. The line of best fit has the equation CCI = −0.0031ΔBDFE + 1.04, and has an R^2 value of 0.95.

substrate (or, if relevant, rearranged product) and chain carrier *hydrides*.

$$\text{agent}-\text{H} + \text{substrate}^\bullet \xrightarrow{\Delta G_e} \text{agent}^\bullet + \text{substrate}-\text{H} \qquad (2)$$

$$\Delta G_e = \text{BDFE}(\text{agent}-\text{H}) - \text{BDFE}(\text{substrate}-\text{H})$$

This step is favored thermodynamically if the agent makes a weaker bond with hydrogen than does the corresponding organic substrate. The overall process, as obtained by summing reactions c to e, is given by eq 3 if the reaction is a pure dehalogenation, where the ΔBDFE measures the relative strengths of the halide and hydride bonds of a given species.

$$\text{agent}-\text{H} + \text{substrate}-\text{X} \xrightarrow{\Delta G_{c-e}} \text{agent}-\text{X} + \text{substrate}-\text{H} \qquad (3)$$

$$\begin{aligned}\Delta G_{c-e} &= \{\text{BDFE}(\text{substrate}-\text{X}) - \text{BDFE}(\text{substrate}-\text{H})\} \\ &\quad - \{\text{BDFE}(\text{agent}-\text{X}) - \text{BDFE}(\text{agent}-\text{H})\} \\ &= \Delta\text{BDFE}(\text{substrate}) - \Delta\text{BDFE}(\text{agent})\end{aligned}$$

When an accompanying rearrangement occurs, this expression will contain an additional correction due to the differing stabilities of the substrate and product radicals in reaction d. In either case the overall process becomes more thermodynamically favored as the agent makes a stronger bond with the halogen compared with the hydrogen. As a minimal thermodynamic requirement, the difference in the agent−X and agent−H BDFEs (i.e., ΔBDFE for the agent) should exceed the corresponding difference in the substrate halide and hydride BDFEs. This leads us to suggest that a simple quantitative measure of the thermodynamic efficiency of the chain carrier is the ratio of its halide to hydride bond dissociation free energies, which we call the "chain carrier index" (CCI).

$$\text{CCI} = \frac{\text{BDFE}(\text{agent}-\text{X})}{\text{BDFE}(\text{agent}-\text{H})} \qquad (4)$$

This ratio shows a good correlation with the corresponding ΔBDFE value (see Figure 1),[10] and has the added advantage of being dimensionless and, as we show shortly, relatively independent of solvent or temperature. Of course both this ratio and the ΔBDFE only measure the overall thermodynamic efficiency of the process, rather than its kinetic efficiency. We will therefore perform additional kinetic studies on selected chain carrier agents using isopropyl bromide as our typical organic substrate.

dx.doi.org/10.1021/jo102368v |*J. Org. Chem.* 2011, 76, 1715–1726

Computational Procedures. Standard ab initio molecular orbital theory[11] and density functional theory[12] calculations were carried out with GAUSSIAN 03[13] and MOLPRO 2002.6.[14] Calculations were performed at a high level of theory, chosen on the basis of a recent assessment study for radical thermochemistry.[15] Further comparisons between theory and experiment are provided as part of the present work. Geometries of all molecules were optimized at the B3LYP/6-31+G(d) level of theory, and frequency calculations were also carried out at this level to ensure that convergence to a local minimum had been achieved. All thermochemical corrections and zero-point vibrational energies were calculated by using the B3LYP/6-31+G(d) geometries and frequencies, and the latter were scaled by the standard B3-LYP/6-31G(d) scale factors.[16] For species containing the third row atoms, Ge, As, and Br, we adopted Rassolov's 6-31+G(d)[17] rather than the default version in Gaussian. Rassolov's 6-31+G(d) basis set is consistent with first and second row atoms, while the default Gaussian 6-31+G(d) basis set is not. For species containing fourth and fifth row atoms, Sn, Sb, Pb, and Bi, LAN2DZdp[18] with an effective core potential (ECP) was used instead of 6-31+G(d).

Improved energies were calculated by using a modified version of G3(MP2)-RAD,[19] G3(MP2)-RAD(+), in which calculations with the 6-31G(d) basis set were replaced by corresponding 6-31+G(d) calculations, or LANL2DZdp with ECP for fourth and fifth row atoms. G3MP2Large was replaced by aug-cc-pVTZ-PP with effective core potential for fourth and fifth row atoms.[20] G3(MP2)-RAD is a high-level composite procedure that approximates coupled cluster energies [URCCSD(T)] with a large triple-ζ basis set, using additivity approximations. This method has been demonstrated to reproduce the experimental heats of formation of a variety of open- and closed-shell species to within approximately 1 kcal mol^{-1},[18] and was recently shown to reproduce a large test set of experimental bond dissociation energies to within chemical accuracy.[21] In the present work we use the "(+)" version to allow for a better treatment of the anionic species in the test set.

For the larger molecules (e.g., tributyltin hydride (Bu_3SnH) and tris(trimethylsily)silane ($(TMS)Si_3H$)), it was necessary to use an ONIOM-based procedure to approximate the G3(MP2)-RAD(+) energies. In the ONIOM method of Morokuma and co-workers,[22] one first defines a "core" section of the reaction that typically includes all forming and breaking bonds and principal substituents attached to them. In forming the core system, the deleted atoms are replaced by hydrogens, chosen so that the core provides a good chemical model of the reaction center. The core system was studied at both the high (G3(MP2)-RAD(+)) and lower level of theory, while the full system was studied only at the lower level of theory (ROMP2/G3MP2large). The G3(MP2)-RAD(+) energy of the full system was then approximated as the sum of the high level energy for the core system and the remote substituent effect, as measured at the lower level of theory. The accuracy of this approach results from the ability of ROMP2/G3MP2large to model the remote substituent effect accurately.[15]

Having obtained the energies, geometries, and frequencies, free energies in the gas phase were calculated by using the standard textbook formulas for the statistical thermodynamics of an ideal gas under the harmonic oscillator/rigid rotor approximation.[23,24] To obtain free energies in solution, free energies of solvation for the studied molecules in water, acetonitrile, toluene, dimethyl sulfoxide (DMSO), and tetrahydrofuran (THF) were calculated by using the conductor-like polarizable continuum model (CPCM)[25] at the B3-LYP/6-31+G(d) level of theory. The radii of the united atom topological model, optimized for the B3-LYP level of theory (UAKS), have been chosen for the determination of solvation energies; the remaining parameters in the CPCM model were kept at their default values in GAUSSIAN.[13] Unless otherwise noted, all geometries of the studied species were optimized fully at the B3-LYP/6-31+G(d) level of theory. All solvation energy calculations were performed using the SCFVAC keyword in Gaussian so that the solvation energy $\Delta G(\text{solv})$ instead of the total free energy in the solvent $\Delta G(\text{soln})$ could be extracted and combined with higher level calculations of the free energy in gas phase $\Delta G(\text{g})$ via a thermodynamic cycle as follows:

$$\Delta G(\text{soln}) = \Delta G(\text{g}) + \Delta G(\text{solv}) + \Delta nRT \ln(RT/P^\circ) \qquad (5)$$

The correction term in this equation, $\Delta nRT \ln(RT/P^\circ)$ (where P° is the standard pressure in the gas-phase calculations and Δn is the change in the number of moles of solvated species in the reaction and is equal to 1 in all the halide and hydride bond dissociation reactions), is needed to account for the passage from 1 atm (g) to 1 mol/L (soln).

For selected reactions, the gas-phase rate constants for the bromine abstraction and hydrogen donation reactions at 298.15 K were calculated via standard transition state theory, in conjunction with the rigid rotor/harmonic oscillator approximation. A previous study of chain transfer in ethylene polymerization has indicated that the use of this approximation should not introduce significant error in the frequency factors for such reactions.[26] The energies, geometries, and free energies of the transition structures were calculated in the same manner used for the stable species (described above). However, for a small number of explicitly noted reactions BMK/6-31+G(d) geometries and frequencies were used in place of B3-LYP/6-31G(d) as the saddle points for the reactions could not be located at the latter level of theory. The scale factors for the BMK frequencies were taken from Merrick et al.[27] For the hydrogen transfer reactions, corrections for quantum mechanical tunneling were calculated by using the Eckart tunneling method.[28] In this method, the minimum energy path for the reaction is approximated by using an Eckart function, for which the one-dimensional Schrödinger equation has an analytical solution. In the present work we fitted the Eckart function to the curvature of the minimum energy path of the reaction at the transition structure, as measured by using the imaginary frequency.[29]

To assist in the qualitative analysis of the results, the charge distribution of the halogen atom in each of the stable molecules was calculated by using Mulliken population analysis on fully optimized geometries at the B3-LYP/6-31+G(d) level of theory.

RESULTS AND DISCUSSION

R−H, R−Cl, and R−Br bond dissociation free energies (BDFEs) were calculated in both the gas phase (at 298.15K and 353.15K) and solution (at 298.15 K) for a wide variety of R-groups, as shown in Schemes 2 and 3. The carbon-centered species in Scheme 2 were chosen to encompass a variety of polar and steric properties, as well as to include selected synthetically accessible and useful molecules. The noncarbon-centered species in Scheme 3 included commonly used radical reducing agents containing tin, phosphorus, and silicon, as well as a number of novel compounds and several homologous series. For the

Scheme 2. Carbon-Centered Species Studied[a]

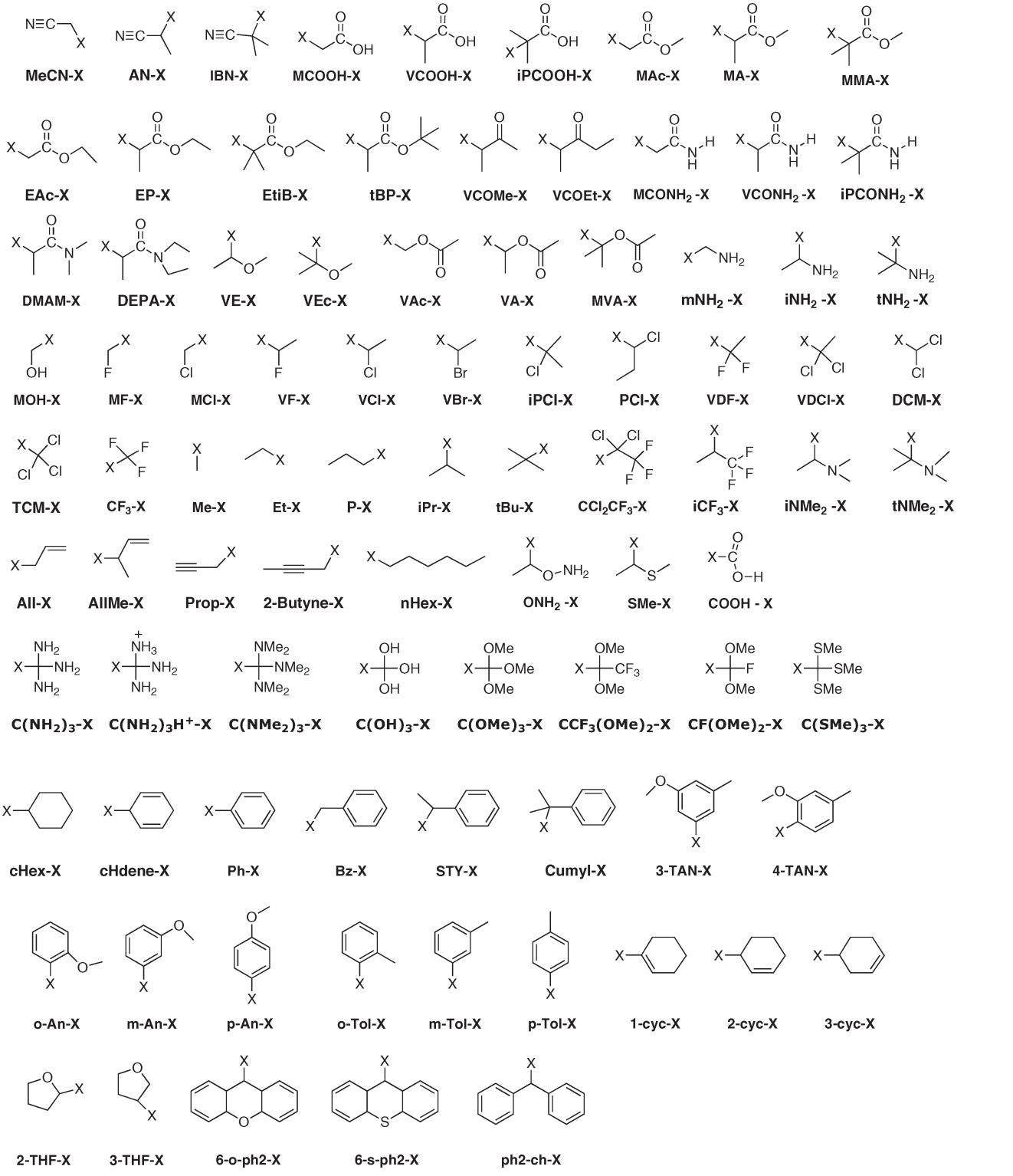

[a] X = H, Cl, Br, or unpaired electron.

solution-phase results a variety of solvents were used, with the solvent for a particular set of R−H and R−X BDFEs chosen so that the species would be soluble. The BDFEs were then used to evaluate the chain carrier index (CCI = BDFE(R−X)/BDFE (R−H)), as well as the hydride and halide BDFE difference (ΔBDFE = BDFE(R−H) − BDFE(R−X)). Table 1 shows the 298.15 K gas-phase free energy BDFEs for each species and corresponding CCI and ΔBDFE values; a full listing of the BDFEs and associated CCIs under all studied conditions is provided in the Supporting Information.

Scheme 3. Noncarbon-Centered Radical Reducing Agents Studied[a]

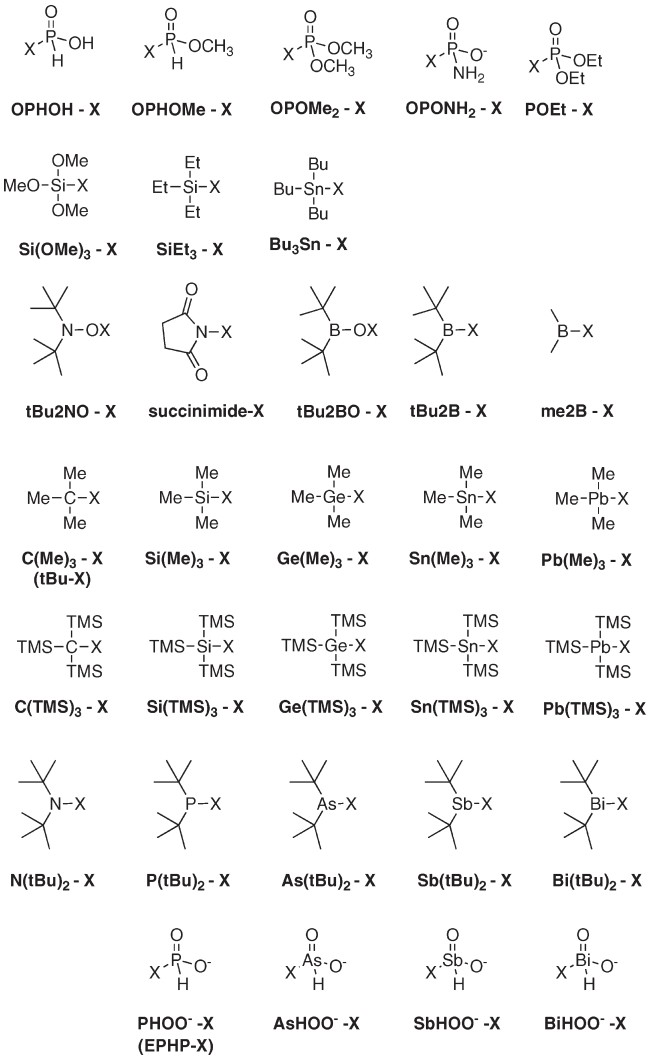

[a] X = H, Cl, Br, or unpaired electron. TMS stands for trimethylsilyl.

Before proceeding to analysis of the data, we note that, for a subset of the studied systems, experimental 298.15 K gas-phase bond dissociation *enthalpies* (BDEs) have been reported and these can be used to test the reliability of the computational data.[30] A full listing of calculated and corresponding experimental BDEs are provided in Table S5 of the Supporting Information; a summary of the results is provided in Figure 2. It is clear from this figure that, consistent with our recent study of radical stability,[21] the chosen level of theory is able to model bond energies accurately for the vast majority of the studied systems. Moreover, in the case of the largest outliers in this figure (the succinimide BDEs), the reported experimental data may be unreliable, given that alternative experimental estimates of the succinimide−H BDEs (and hence the corresponding radical heats of formation that may be used to obtain the other BDEs) cover a 100 kJ mol^{-1} range. When these succinimide BDEs are omitted (and all other experimental data are accepted at face value), the mean absolute deviation of theory versus experiment is just 6.0 kJ mol^{-1}, which is close to the reported average experimental uncertainty of the same data, 5.0 kJ mol^{-1}.

Effect of Reaction Conditions. To examine the effects of solvent and temperature on the CCI values, Figure 3a shows a plot of the 353.15 K gas-phase CCI values against the corresponding 298.15 K gas-phase CCI values; Figure 3b compares the corresponding 298.15 K solution- and gas-phase CCIs. It is seen from Figure 3a that temperature has very little effect on the CCI value. This is not surprising, as the thermal contribution to the relative R−X and R−H BDFEs is likely to be very similar, differing principally in the translational entropy change associated with losing a hydrogen versus a heavier halogen. With the exception of the charged species, solvent also has a surprisingly small effect on the CCI, with most of the data closely distributed around the line $y = x$ in Figure 3b. This is despite the fact that the solvent was itself varied among the data set according to the solubility of the studied species and thus included a variety of nonpolar and polar solvents. Bearing in mind that the CCI is the ratio of an R−Cl or R−Br BDFE to an R−H BDFE, this implies that solvent effects on these bond energies are relatively similar. As we explain below, the principal difference between corresponding R−X and R−H bond energies is the larger covalent−ionic resonance contribution to the R−X bond energy of the halide. As demonstrated by Shaik, Hiberty, and co-workers[31] for related compounds such as CH_3−Cl and SiH_3−Cl this resonance is not accompanied by an increased dipole moment, and is therefore relatively insensitive to solvent effects, which is indeed consistent with our results in Figure 3b. In practical terms, these results imply that, *provided an appropriate inert solvent is used*, the thermodynamic efficiency of a neutral chain carrier is solvent-independent. Given this relative insensitivity to the reaction conditions, for the remainder of this work we focus on the 298.15 K gas-phase values except when studying the small set of Group 15 charged species.

Noncarbon-Centered Chain Carriers. Examining the CCI values in Table 1, it is obvious that the widely used radical reducing agents like EPHP, $Si(TMS)_3H$, and Bu_3SnH have CCI values that are considerably larger than those for carbon-centered species, consistent with their known success in effecting radical dehalogenation of organic substrates. It is also seen that, with the notable exception of $(tBu)_2B$−H, the chain carriers centered with other second row elements (such as O or N) also have significantly lower CCIs than their heavier analogues. To illustrate these trends more systematically, Figure 4 shows the changes to 4 different homologous series of CCIs as one moves down a column of the Periodic Table. Panels a and b of Figure 4 show CCIs for two series of Group 14 compounds: panel a shows species with methyl substituents (chosen to mimic chain carriers such as H−$SiEt_3$ or H−$PbBu_3$); and panel b shows the same species but with trimethylsilyl groups (as in the known chain carrier H−$Si(SiMe_3)_3$). Figures 4c and 4d show CCIs for two Group 15 homologous series: panel c shows species with alkyl groups (this time with *tert*-butyl to help stabilize the chain carrier); and panel d shows analogues of the active species in the known chain carrier EPHP (i.e., H−$PH(O)O^-$). Since these latter chain carriers are charged and subject to significant solvent effects, aqueous results are shown for Figure 4d.

From Figure 4, it is seen that in all 4 series there is a general increase in the CCI as one moves down a column of the periodic table, though the increase from the second to the third rows (e.g., from C to Si, or N to P) is much more significant than the subsequent increases. These trends are similar for corresponding chlorides and bromides, though in each case the chloride CCIs are significantly greater than the corresponding bromide ones.

dx.doi.org/10.1021/jo102368v |*J. Org. Chem.* 2011, 76, 1715–1726

Table 1. Gas-Phase Bond Dissociation Free Energies (BDFEs; kJ mol^{-1}),[a] Chain Carrier Indices (CCI = BDFE(R−X)/BDFE(R−H)), and Relative BDFEs (ΔBDFE = BDFE(R−H) − BDFE(R−X)) at 298.15 K

	R−H	R−Cl			R−Br		
R−X[b]	BDFE	BDFE	CCI-Cl	ΔBDFE	BDFE	CCI−Br	ΔBDFE
MeCN−X	367	262	0.716	104	209	0.569	158
AN−X	349	259	0.744	89	203	0.582	146
IBN−X	335	259	0.771	77	200	0.596	136
MCOOH−X	380	284	0.746	97	228	0.601	152
VCOOH−X	356	274	0.769	82	218	0.612	138
iPCOOH−X	334	264	0.792	69	205	0.615	128
MAc−X	379	284	0.749	95	229	0.605	150
MA−X	355	277	0.779	79	221	0.622	135
MMA−X	335	268	0.801	67	210	0.626	125
EAc−X	378	285	0.753	93	230	0.609	148
EP−X	354	278	0.783	77	222	0.625	133
EtiB−X	336	271	0.807	65	212	0.632	124
tBP−X	352	280	0.796	72	224	0.638	128
VCOMe−X	351	278	0.792	73	221	0.629	130
VCOEt−X	355	282	0.796	72	224	0.630	131
MCONH2−X	383	299	0.781	84	242	0.631	141
VCONH2−X	357	289	0.809	68	229	0.642	128
iPCONH2−X	350	291	0.830	59	228	0.652	122
DMAM−X	354	285	0.806	69	229	0.646	125
DEPA−X	350	285	0.812	66	229	0.652	122
VE−X	359	316	0.878	44	255	0.710	104
VEC−X	362	298	0.823	64	255	0.703	108
VAc−X	378	305	0.807	73	245	0.650	132
VA−X	370	309	0.835	61	247	0.669	122
MVA−X	374	306	0.820	67	243	0.652	130
mNH$_2$−X	355	304	0.857	51	246	0.693	109
iNH$_2$−X	350	308	0.882	41	249	0.711	101
tNH$_2$−X	349	313	0.898	35	252	0.723	96
MOH−X	367	310	0.844	57	249	0.678	118
MF−X	384	316	0.821	69	253	0.659	131
MCl−X	374	291	0.778	83	233	0.622	141
VF−X	378	318	0.841	60	255	0.674	123
VCl−X	369	294	0.798	74	234	0.635	135
VBr−X	374	295	0.789	79	235	0.629	139
iPCl−X	363	293	0.808	70	233	0.642	130
PCl−X	367	294	0.801	73	234	0.638	133
VDF−X	386	321	0.832	65	254	0.658	132
VDCl−X	360	274	0.762	86	212	0.590	148
DCM−X	364	276	0.758	88	215	0.592	148
TCM−X	354	256	0.723	98	195	0.549	160
CF$_3$−X	412	324	0.786	88	256	0.621	156
Me−X	399	315	0.789	84	260	0.652	139
Et−X	378	312	0.826	66	255	0.675	123
P−X	382	315	0.824	67	258	0.675	124
iPr−X	368	314	0.853	54	255	0.692	113
tBu−X	363	316	0.870	47	255	0.702	108
CCl$_2$CF$_3$−X	365	262	0.717	103	203	0.557	162
iCF$_3$−X	386	301	0.779	85	242	0.627	144
iNMe$_2$−X	349	309	0.886	40	255	0.729	94
tNMe$_2$−X	347	310	0.895	36	255	0.735	92
All−X	332	254	0.766	78	199	0.600	133
AllMe−X	317	253	0.798	64	196	0.618	121
Prop−X	347	256	0.738	91	202	0.581	145
2-butyne−X	333	256	0.768	77	201	0.604	132
nHex−X	380	315	0.830	65	259	0.681	121
ONH$_2$−X	374	327	0.874	47	266	0.712	108
SMe−X	351	284	0.808	67	230	0.654	121
COOH−X	361	310	0.858	51	248	0.687	113
C(NH$_2$)$_3$−X	352	305	0.865	47	242	0.687	110
C(NH$_2$)$_2$NH$_3^+$−X	[c]	286			223		

	R−H	R−Cl			R−Br		
R−X[b]	BDFE	BDFE	CCI-Cl	ΔBDFE	BDFE	CCI−Br	ΔBDFE
C(NMe$_2$)$_3$−X	345	278	0.807	67	−[c]		
C(OH)$_3$−X	365	313	0.859	52	248	0.681	116
C(OMe)$_3$−X	364	321	0.881	43	260	0.714	104
CF(OMe)$_2$−X	378	320	0.847	58	255	0.674	123
CCF$_3$(OMe)$_2$−X	370	303	0.820	66	239	0.647	130
C(SMe)$_3$−X	319	249	0.783	69	190	0.597	128
cHex−X	369	323	0.874	46	264	0.716	105
cHdene−X	284	224	0.788	60	169	0.594	115
Ph−X	439	370	0.842	69	308	0.703	130
Bz−X	348	268	0.769	80	213	0.612	135
STY−X	332	267	0.804	65	209	0.630	123
Cumyl−X	332	271	0.817	61	210	0.634	121
3-TAN−X	434	369	0.850	65	308	0.709	126
4-TAN−X	446	373	0.837	73	314	0.703	133
o-An−X	436	370	0.849	66	309	0.709	127
m-An−X	435	361	0.831	73	301	0.693	133
p-An−X	441	373	0.846	68	312	0.708	129
o-Tol−X	436	371	0.852	65	311	0.713	125
m-Tol−X	438	370	0.845	68	308	0.705	129
p-Tol−X	436	373	0.854	64	309	0.708	127
1-cyc−X	421	365	0.868	55	304	0.723	116
2-cyc−X	313	254	0.809	60	196	0.626	117
3-cyc−X	375	319	0.853	55	261	0.696	114
2-THF−X	354	314	0.887	40	254	0.716	101
3-THF−X	371	310	0.837	60	251	0.678	119
6-*o*-ph2−X	285	220	0.773	65	164	0.576	121
6-s-ph2−X	287	218	0.761	68	164	0.572	123
ph$_2$-ch−X	320	246	0.768	74	188	0.587	132
OPHOH−X	331	359	1.084	−28	289	0.873	42
OPHOMe−X	329	361	1.097	−32	292	0.887	37
OPOMe2−X	353	375	1.063	−22	306	0.866	47
OPONH2−X	335	402	1.198	−67	344	1.024	−8
POEt−X	354	372	1.050	−18	302	0.853	52
Si(OMe)$_3$−X	373	467	1.254	−94	394	1.057	−21
SiEt$_3$−X	356	456	1.280	−100	391	1.097	−35
Bu$_3$Sn−X	287	393	1.372	−107	340	1.186	−53
tBu2NO−X	243	86	0.355	156	54	0.221	189
succinimide−X	505	307	0.608	198	272	0.538	233
tBu$_2$BO−X	382	104	0.272	278	78	0.204	304
tBu$_2$B−X	396	479	1.209	−83	403	1.016	−6
Me$_2$B−X	394	484	1.228	−90	410	1.040	−16
C(Me)$_3$−X	369	315	0.856	53	254	0.690	114
Si(Me)$_3$−X	357	454	1.272	−97	385	1.077	−28
Ge(Me)$_3$−X	326	407	1.247	−81	348	1.066	−22
Sn(Me)$_3$−X	289	394	1.365	−105	340	1.177	−51
Pb(Me)$_3$−X	244	346	1.420	−102	295	1.212	−52
C(TMS)$_3$−X	368	287	0.780	81	238	0.648	129
Si(TMS)$_3$−X	312	394	1.264	−82	337	1.079	−25
Ge(TMS)$_3$−X	287	361	1.256	−73	310	1.081	−23
Sn(TMS)$_3$−X	284	383	1.350	−99	337	1.186	−53
Pb(TMS)$_3$−X	275	380	1.381	−105	334	1.214	−59
N(tBu)$_2$−X	365	179	0.491	186	129	0.353	236
P(tBu)$_2$−X	304	318	1.046	−14	257	0.846	47
As(tBu)2−X	275	307	1.119	−33	253	0.921	22
Sb(tBu)2−X	248	323	1.300	−75	270	1.087	−22
Bi(tBu)$_2$−X	225	313	1.390	−88	264	1.171	−39
PH(O)O$^-$−X	314	405	1.290	−91	347	1.104	−33
AsH(O)O$^-$−X	258	351	1.359	−93	297	1.152	−39
SbH(O)O$^-$−X	223	337	1.508	−113	284	1.272	−61
BiH(O)O$^-$−X	148	271	1.839	−124	224	1.518	−76

[a] Calculated at the G3(MP2)-RAD(+)//B3-LYP/6-31+G(d) level of theory, using the harmonic oscillator approximation. Corresponding gas-phase values at 353.15 K and solution-phase values at 298.15 K are provided in the Supporting Information. [b] All carbon-centered structures are defined in Scheme 2 and all noncarbon-centered species are defined in Scheme 3. [c] Could not be calculated as relevant species were unstable to dissociation (C(NH$_2$)$_2$NH$_3^+$ radical cation loses NH$_3^+$; C(NMe$_2$)$_3$-Br loses Br$^-$).

dx.doi.org/10.1021/jo102368v |*J. Org. Chem.* 2011, 76, 1715–1726

Bearing in mind that the CCI is a measure of the relative R−X to R−H BDFEs, the large values of the CCIs for the heavier radical reducing agents imply that they make proportionally stronger bonds with halogens than with hydrogen, when compared with the corresponding lighter species.

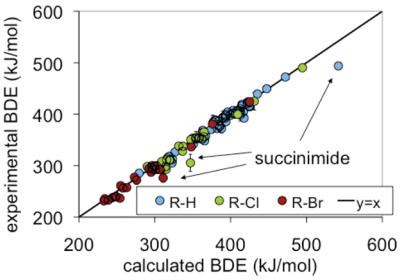

Figure 2. Comparison of theory and experimental BDE.

The broad trends in halide bond strength are already well-known. For example, in the 1990s, Shaik, Hiberty, and co-workers analyzed the trends in the MH_3−Cl (M = C, Si, Ge, Sn, and Pb) bond energies of the Group 14 chlorides using breathing orbital valence bond theory (BOVB).[31] They argued that the bond energies, which increased significantly down the column from C to Si before slowly decreasing again, were the result of the resonance between the covalent and ionic configurations of the halide bond. Thus, within their studied series, the ionic configurations are progressively stabilized down the column by electrostatic and hyperconjugative effects; the covalent configurations are progressively destabilized; for this series the ionic and covalent configurations are closest in energy (and hence most easily undergo resonance) when the bonding center is the Si atom.

If we examine our own data in the light of these findings, we first note that the CCI depends not only on the strength of the halide bond per se but on its strength relative to the corresponding hydride bond. Since hydrogen is a poor electron acceptor, the

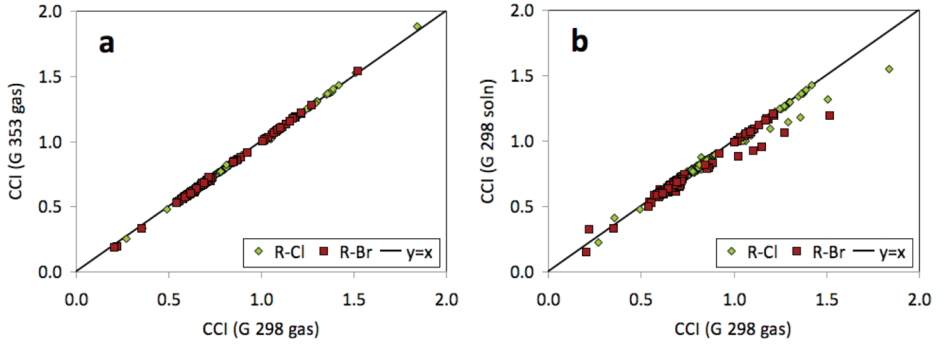

Figure 3. Effect of (a) temperature and (b) solvent on the CCI values for the full test set. Outliers in part b are X−$OPONH_2$ and all anionic species (X−$PH(O)O^-$, X−$AsH(O)O^-$, X−$SbH(O)O^-$, and X−$BiH(O)O^-$).

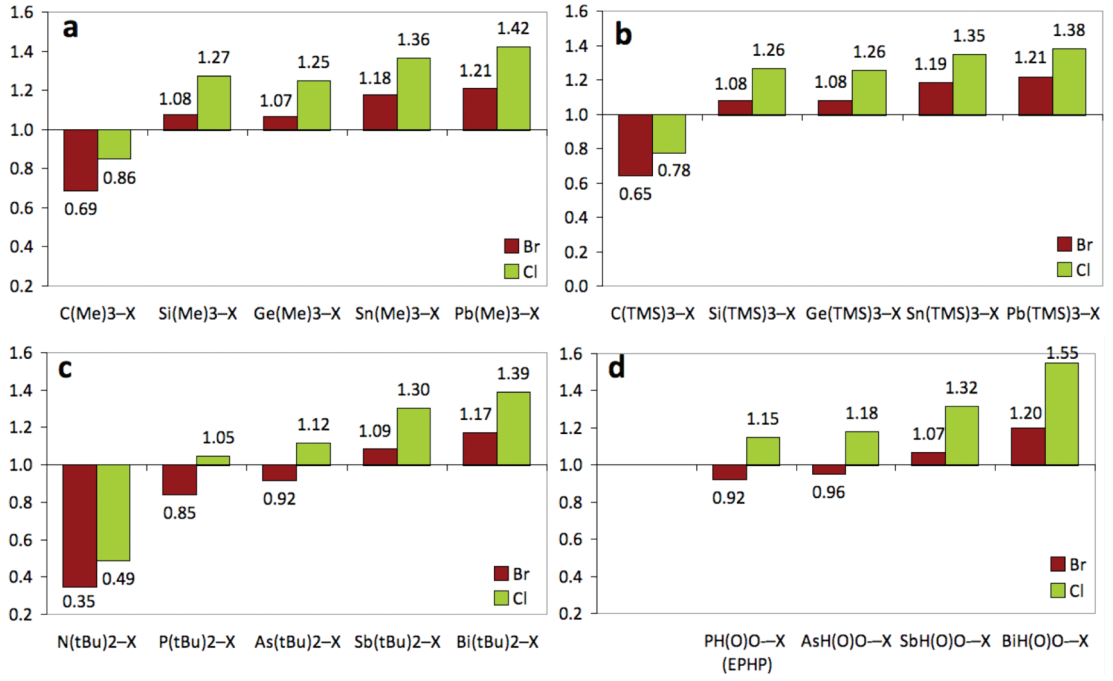

Figure 4. The 298.15 K CCIs for selected group 14 and group 15 homologous series. In panels a−c the effects of solvation are minor and gas-phase data are shown; for the charged species in part d the solvent effect is more significant and hence aqueous CCIs are displayed as being more relevant to synthetic applications.

dx.doi.org/10.1021/jo102368v |J. Org. Chem. 2011, 76, 1715–1726

polar−ionic contribution is likely to be much less significant in these compounds and the bond strengths will depend largely on overlap, with the heavier atoms making weaker bonds with hydrogen compared with lighter atoms. The net result of these trends in halide and hydride bond strengths is that the CCI generally increases down a column of the periodic table. However, due to charge-shift bonding, the increase from the second to the third row is much steeper than the subsequent changes, as is observed in Figure 4. The increased CCIs for chlorides versus corresponding bromides is also consistent with the concept of charge-shift bonding in that the ionic contribution is generally likely to be more significant for the chlorides than the bromides, due to the greater electronegativity of the respective halogen atoms. Among the other compounds studied, the substituent effects are broadly consistent with the concept of charge-shift bonding. For example, inclusion of the lone pair donor oxygen substituents (as in Figure 4d) instead of alkyl groups (as in Figure 4c) on the Group 15 compounds leads to increased CCIs due to the enhanced stabilization of the ionic configuration.

From a practical perspective, these results suggest that bismuth-centered compounds would be worth further investigation as tin-free radical reducing agents. Not only are the CCIs for the studied compounds ($H-Bi(tBu)_2$ and $H-BiH(O)O^-$) higher than those for existing species, but unlike other heavy metals, most bismuth compounds are relatively nontoxic.[32] Among the other compounds studied, $H-B(tBu)_2$ and related compounds might also be worthy of further study. This compound has a surprisingly high CCI compared with compounds containing carbon (or other second row elements such as oxygen or nitrogen) as their radical center, indicating that this compound could (at least in principle) function as a radical reducing agent for organic species. Unlike the other elements studied, boron is generally an effective σ donor and this probably explains the enhanced relative strength of its halide bond. In any case, given that radical-based organic transformations are sometimes carried out on borane adducts of the substrates, these results suggest the participation of the borane as a radical chain carrier might need to be considered as a possible side reaction in some cases.

Carbon-Centered Chain Carriers. Finding an effective carbon-based chain carrier agent would be an exciting prospect; not only would such a species be free from toxic heavy metals such as lead, but it could also be potentially cheaper, and more easily made and handled. However, finding a suitable species is a considerable challenge as any universal chain carrier would have to have a CCI sufficiently large to exceed that of the typical carbon-centered substrates encountered in synthesis. Unfortunately, the principal factor governing the CCI is the nature of the bonding atoms themselves; by contrast, differences due to the substitution pattern are relatively small. Nonetheless, it is worth understanding these differences and exploring whether they could be exploited to design an effective carbon-centered chain carrier, or at least be used to exclude unsuitable species from further consideration

To help analyze the effects of substituents on the CCIs in Table 1, Figure 5 shows the corresponding chloride and bromide CCIs for a representative set of $X-CH(CH_3)R$ species, along with the prototypical sp^2 species X−COOH and X−Ph and the prototypical cyclic species cHex−X. From this figure it is clear that the CCIs for the chlorides are systematically higher than those of the bromides. This reflects the tendency of carbon to form stronger bonds with chlorine versus bromine due to better overlap and stronger polar−covalent resonance interactions. Within each series there is a modest increase in the CCI as the electron-donating ability of the

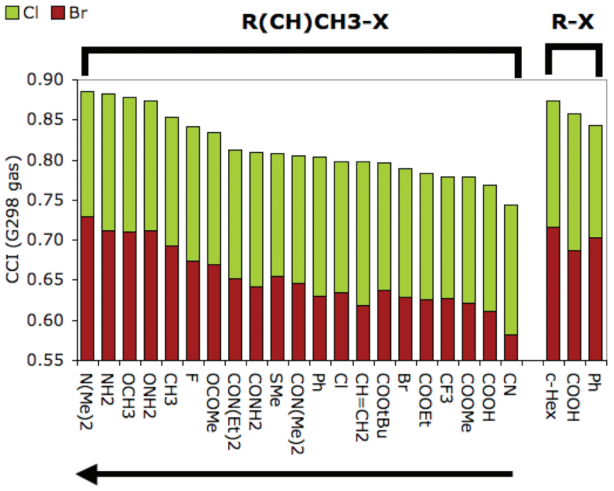

Figure 5. Effect of halogen (X = Br, Cl) and substituents (R) on the CCI (gas phase, 298.15 K) for $RCH(CH_3)X$ and R−X (gas-phase 298.15 K) for organic chlorides and bromides. The $RCH(CH_3)X$ set is arranged according to the electronegativity of X, with the arrow showing increasing electron donation capacity.

R-group increases from electron-withdrawing groups such as cyano or carbonyl substituents through to the lone pair donor amino or alkoxy groups. This is also consistent with the increased ability of the electron-donating groups to help stabilize the $alkyl^+$ X^- ionic configuration of the alkyl halide bond. The cyclic species cHex−X shows a slightly higher CCI (0.874 for X = Cl) than the analogous noncyclic secondary carbon-centered species (iPr−X, CCI = 0.853 for X = Cl) while the sp^2 species H−COOH (0.858) and H−Ph (0.842) have slightly lower values, though all are still within the same basic range.

From Table 1 it is also seen that the CCI generally increases from primary to tertiary in the series $X-CH_2R$, $X-CH(CH_3)R$, and $X-C(CH_3)_2R$. This is illustrated in Figure 6a for a representative set of bromides; similar trends are observed for the chlorides though the CCIs are systematically higher in this case. In other words the halide bond is strengthened compared with the hydride bond as the alkyl group becomes more substituted. These trends, which have been noted previously for related species such as Me−F, Et−F, iPr−F, and tBu−F,[33] can be understood in terms of the same charge-shift bonding arguments outlined above. Thus, the halide bond is strengthened by resonance between its covalent (e.g., $X\cdot\cdot CH_2R$) and ionic forms (e.g., $X^{-+}CH_2R$), and this resonance is expected to strengthen as the carbon center is substituted with additional alkyl groups, because the additional β C−H bonds help to hyperconjugatively stabilize the ionic configuration. In support of this we note that, within each series, there is a reasonable correlation between the enthalpic component of the CCI and the degree of charge localization on the halogen (see Figure 6b). The only major exception is the $H-C(OCOCH_3)RR'$ series in which anomeric effects may be a complicating factor (see Figure 6a,b).

On the basis of this thermodynamic analysis, one would expect that the best (neutral) candidates for carbon-centered chain carriers would be those substituted with electron-donating groups such NR_2 or OR. While their CCIs are considerably lower than typical noncarbon-centered chain carriers such as EPHP, $H-Si(SiMe_3)$, and $H-Sn(Bu)_3$, they are about 10% higher than most of the other studied carbon-centered species. In other words, on a thermodynamic basis at least, such species

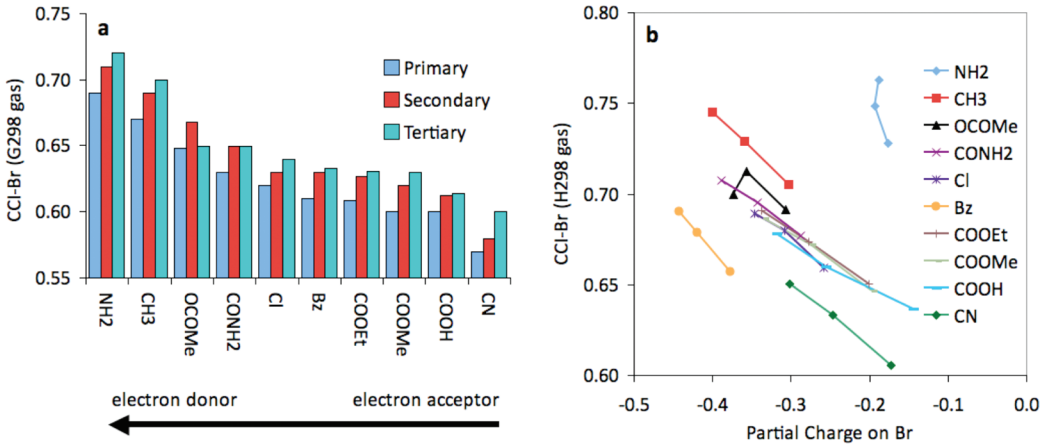

Figure 6. (a) Effect of degree of substitution on the 298.15 K gas-phase CCI−Br on primary ($Br-CH_2R$), secondary ($Br-CH(CH_3)R$), and tertiary ($Br-C(CH_3)_2R$) carbon centers. (b) Plot of partial mulliken charge on Br against the enthalpic component of the 298.15 K gas-phase CCI-Br for various functional groups on primary, secondary, and tertiary carbon centers.

would function as chain carriers for the dehalogenation of most types of organic substrates. Of course, in choosing a suitable reagent other considerations have to be taken into account. The amine in particular is not likely to be successful in situations where it can be protonated as the proton would then compete for the nitrogen lone pair. Moreover, we found that the protonated species $HC(NH_3)(NH_2)_2^+$ would in any case be unsuitable as a chain carrier as the radical cation is unstable to the loss of NH_3.

Kinetic Considerations. As is clear from Scheme 1, dehalogenation is a complex multistep process and the overall yield will depend not only on the thermodynamics of the propagation steps, but also on how well these steps compete kinetically with radical−radical termination and other side reactions. Under the steady state assumption, the overall rate of a pure dehalogenation reaction can be represented by the following equation (see Appendix S1 of the Supporting Information for the derivation).

$$-\frac{d[\text{R–X}]}{dt} = \frac{d[\text{R–H}]}{dt} = \sqrt{\frac{fk_a[\text{initiator}]}{k_f}} \frac{k_c k_e[\text{agent–H}][\text{R–X}]}{\sqrt{k_e^2[\text{agent–H}]^2 + k_c k_e[\text{agent–H}][\text{R–X}] + k_c^2[\text{R–X}]^2}} \quad (6)$$

In this equation k_a, k_c, k_e, and k_f are the rate coefficients for reactions a, c, e, and f in Scheme 1, f represents the fraction of initiator derived radicals that escape the solvent cage and proceed to reaction b in Scheme 1, and it is assumed for simplicity that the various bimolecular termination reactions all occur with the same diffusion-controlled rate coefficient k_f. Although in the general case the overall reaction rate depends on the rate coefficients of both propagation steps (and scales roughly with their geometric mean when the rate coefficients are not too dissimilar), if one step is considerably slower than the other it can be shown that the overall rate effectively only depends on the slowest propagation step (see Appendix S1 for further details).[34] This is in contrast to the thermodynamic situation, where it is the overall free energy change that determines whether a process is feasible or not, and where one individual step can be thermodynamically disfavored provided the other steps can provide a sufficient thermodynamic driving force to compensate. For kinetic efficiency it is essential that *both* propagation steps are sufficiently kinetically favored.

Table 2. Forward Rate Coefficients for Reactions c and e and Their Geometric Mean in the Dehalogenation of X−CH-$(CH_3)_2$, Using Various Chain Carrier Radicals[a]

chain carrier radical	X	k_c	k_e[b]	$(k_c \times k_e)^{0.5}$
$^{\bullet}PH(O)O^-$ [c] (EPHP)	Br	1.1×10^8	3.2×10^4	1.9×10^6
$^{\bullet}CH(OCH_3)CH_3$ (VE)	Br	2.7×10^2	2.0	2.4×10^1
$^{\bullet}BMe_2$[c]	Br	4.0×10^8	1.4×10^{-2}	2.3×10^3
$^{\bullet}BiH(O)O^-$	Br	2.3×10^{-3}	1.5×10^{10}	5.8×10^3
$^{\bullet}BiH(O)O^-$	Cl	5.7×10^{-8}	1.5×10^{10}	2.9×10^1

[a] Kinetic parameters calculated with G3(MP2)-RAD(+)//B3LYP/6-31+G(d) at 298.15 K in the gas phase. As shown in Scheme 1, reaction c is a halogen abstraction by the chain carrier radical from the organic substrate while reaction e is a hydrogen abstraction from the chain carrier hydride by the organic substrate radical. [b] Includes corrections for quantum-mechanical tunneling. [c] With use of G3-(MP2)-RAD(+)//BMK/6-31+G(d) instead of G3(MP2)-RAD(+)//B3LYP/6-31+G(d) because the saddle point could not be located on the potential energy surface by using the latter.

In this section, we test this kinetic condition for a selection of chain carriers with promising CCIs. Since we now must consider the individual propagation steps, it is necessary to define a "typical" substrate with which to balance the reactions and thereby test the chain carriers in a practical setting. To this end, in the present work, we examined the dehalogenation of isopropyl bromide $Br-CH(CH_3)_2$ using four different types of chain carrier: a known successful chain carrier, EPHP, which we use as a reference; one of the better carbon-centered species studied, $H-CH(OCH_3)CH_3$ (abbreviated as H−VE in Table 1); and two promising noncarbon-centered species, $H-B(CH_3)_2$ and $H-BiH(O)O^-$. For this last chain carrier, the corresponding rate coefficients for dechlorination of $Cl-CH(CH_3)_2$ were also calculated. In all cases the CCIs of the chain carriers exceed those of the corresponding organic substrate and hence they should be thermodynamically suitable. For each studied reaction, the 298.15 K gas-phase rate coefficients were calculated for the hydrogen and halogen abstractions (reactions e and c), and these values and their corresponding geometric mean are listed in Table 2.

As a reference point we note that 298.15 K experimental values of the rate coefficients for hydrogen abstraction from the successful chain carriers, $H-Bu_3Sn$ and $H-Si(TMS)_3$, by

dx.doi.org/10.1021/jo102368v |J. Org. Chem. 2011, 76, 1715–1726

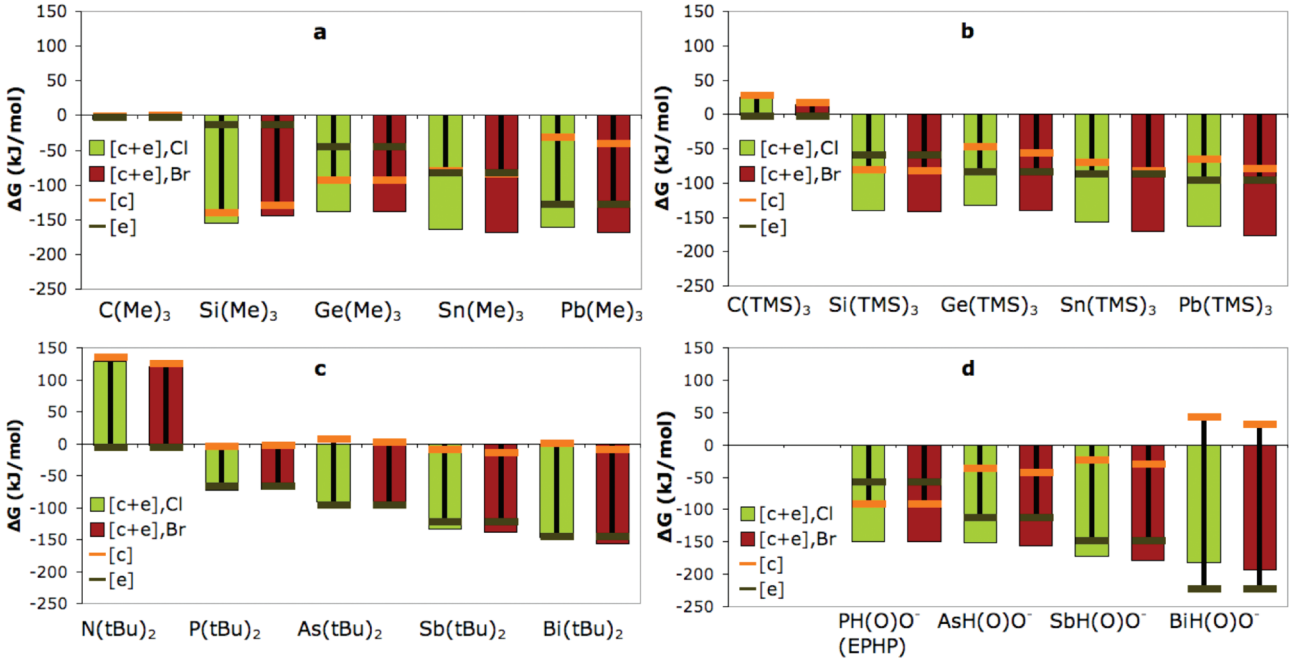

Figure 7. Reaction free energies (ΔG) for reactions c, e, and the overall propagation step (c + e) at 298.15 K for the dehalogenation of X−$CH(CH_3)_2$ (X = Cl or Br) by each of the noncarbon-based agents in Figure 4. As in Figure 4, panels a−c present gas-phase values, while panel d presents values for aqueous solution.

$R_2CH^{\bullet}$ type radicals are 2.3×10^6 and 3.8×10^5 L mol^{-1} s^{-1}, respectively, while rate coefficients for bromine abstraction from the organic bromide by these chain carrier radicals are around 10^8 L mol^{-1} s^{-1}.[35] Their overall reaction rates will thus be limited by their hydrogen abstraction rate coefficients, which fall into the general range of 10^5−10^6 L mol^{-1} s^{-1}. For EPHP, our calculated 298 K gas-phase rate coefficients for bromine abstraction from Br−$CH(CH_3)_2$ and hydrogen donation to $^{\bullet}CH(CH_3)_2$ (i.e., reactions c and e) are 1.1×10^8 and 3.2×10^4 L mol^{-1} s^{-1}. The rate limiting hydrogen abstraction step is thus an order of magnitude below that of H−$Si(TMS)_3$ and two orders of magnitude below that of H−Bu_3Sn. This explains why this chain carrier needs to be used in large stoichiometric excess with high initiator concentrations: such concentration increases are needed to compensate for its lower value of k_e compared with other successful chain carriers. Since yet further concentration increases are undesirable on the grounds of synthetic efficiency, this approximate value of 10^4 L mol^{-1} s^{-1} for either propagation step probably represents a minimal kinetic requirement for any other successful chain carrier.

For the carbon-centered chain carrier, H−$CH(OCH_3)CH_3$, our calculated rate constants for bromine abstraction and hydrogen donation (reactions c and e) in the dehalogenation of Br−$CH(CH_3)_2$ are calculated to be 2.7×10^2 and 2.0 L mol^{-1} s^{-1} respectively, with the latter being rate limiting as expected. Consistent with its considerably lower CCI value, the rate limiting hydrogen abstraction rate coefficient is 3 orders of magnitude below that of EPHP, and the process would therefore require impractical amounts of initiator and/or an even larger stoichiometric excess of chain carrier to achieve reasonable yields. It is also worth noting that, as expected from its low CCI value, the halogen transfer rate coefficient is also well below that of the rate-determining propagation step in successful processes. Any efforts to enhance the hydrogen transfer step by for example stabilizing the resulting carbon-centered radical would only render the halogen transfer step rate limiting instead.

Unfortunately, the compounds with the higher CCI values also fare poorly compared with EPHP. For H−$B(CH_3)_2$ with the same substrate, Br−$CH(CH_3)_2$, the rate coefficients of the bromine abstraction and hydrogen donation propagation steps (reactions c and e) are calculated to be 4.0×10^8 and 1.4×10^{-2} L mol^{-1} s^{-1}, respectively. For this chain carrier the bromine abstraction reaction is considerably faster than that for the carbon-centered species but the hydrogen donation is even slower and this chain carrier would also be impractical from a kinetic perspective. For H−$BiH(O)O^-$ as the agent, the hydrogen abstraction (1.5×10^{10} L mol^{-1} s^{-1}) reaction is so fast as to likely be diffusion limited but the halogen abstraction is now the limiting step and has values that are too low to be practical (2.3×10^{-3} L mol^{-1} s^{-1} for Br and 5.7×10^{-8} L mol^{-1} s^{-1} for Cl).

To help understand why these heavier chain carriers fail on kinetic grounds, Figure 7 shows overall reaction free energies for the propagation reactions of Br−$CH(CH_3)_2$ with the same homologous series chain carriers studied in Figure 4; the corresponding reaction energies for the individual propagation steps are also shown. As might have been anticipated from Figure 1, the trends in the overall free energies mirror those in the CCI values in Figure 4, and the overall reaction free energies for the bismuth compounds are the most exothermic of those studied. However, as might have been anticipated from the kinetic studies, this thermodynamic efficiency is achieved through the strongly exothermic hydrogen step (reaction e), which compensates for the strongly endothermic halogen abstraction step (reaction c). Although not shown in Figure 7, a similar situation exists for the borane except that it is now the halogen abstraction that is highly exothermic. These large differences in thermodynamics for the individual propagation steps are in contrast to the situation for successful chain carriers

dx.doi.org/10.1021/jo102368v |J. Org. Chem. 2011, 76, 1715–1726

such as EPHP, H−Si(TMS)$_3$, and the various tin, lead, and germanium hydrides. In these cases both contributing reactions have similar modest exothermicities, which then enables *both* individual steps to have sufficiently fast rate coefficients.

Although the present boron- and bismuth-centered compounds are not kinetically suitable, they do represent useful starting points for further optimization. As a result of their high CCI values, their non-rate-determining reaction is several orders of magnitude faster than it needs to be in order to mediate the dehalogenation reaction. This provides a large cushion that can be exploited when optimizing the rate of the slower reaction through substitution changes. Thus, for example, in the case of the borane chain carrier, the hydrogen donation reaction could be enhanced by choosing substituents that help to stabilize the corresponding boron-centered radical. This in turn would reduce the rate of the halogen abstraction step, but since this is already extremely fast, this reduction would be unlikely to be enough to affect the overall reaction rate. Indeed, Ueng et al.[36] have recently designed effective borane-based radical chain carriers by modifying the substituents of the borane so as to reduce the hydride bond strength and enhance the hydrogen donation rate. Similar efforts to enhance the halogen abstraction rate of bismuth-centered compounds, this time by reducing the radical stability and/or increasing the strength of the charge-shift bonding, would also be worth further investigation.

CONCLUSION

In the present work we have introduced the chain carrier index, CCI = BDFE(R−X)/BDFE(R−H), as a simple substrate-independent measure of the thermodynamic efficiency of a radical reducing agent (R−H) when used in dechlorination (X = Cl) or debromination (X = Br), and have used high-level ab initio molecular orbital calculations to study the effects of substituents and reaction conditions on the CCI for a broad range of carbon- and noncarbon-centered chain carriers. For a thermodynamically efficient process, the CCI, which is largely solvent and temperature independent, should at least exceed that of the corresponding organic substrate, though for kinetic reasons the CCIs of successful chain carriers tend to be substantially larger. As a rough guideline, values for typical organic substrates tend to fall into the range of 0.7−0.9 for chlorides and 0.55−0.75 for bromides; known successful chain carriers such as EPHP, H−SnBu$_3$, and H−SiTMS$_3$ tend to have CCIs exceeding 1.3 (when defined for use in dechlorination) and 1.1 (when defined for use in debromination).

Successful chain carriers generally maximize the relative strength of their halide (versus hydride bonds) through charge-shift bonding. As a result, the thermodynamic efficiency of a chain carrier tends to increase down the periodic table, and also with the inclusion of stronger electron-donating substituents. Of the compounds studied, the bismuth hydrides such as H−Bi(tBu)$_2$ and H−BiH(O)O$^-$ were the most thermodynamically efficient compounds, closely followed by the other heavy group 14 and 15 hydrides. For the same reasons, lighter compounds such as carbon-, nitrogen-, and oxygen-centered species have relatively stronger hydride versus halide bonds and are generally not thermodynamically capable of effecting radical dehalogenation for organic substrates. In particular, the CCIs of carbon-centered species fall into a relatively narrow range, despite considering a very broad range of substitution changes. Even when the CCI is maximized through inclusion of multiple lone pair donor OMe or NMe$_2$ groups, the thermodynamic driving force for their dehalogenation of other organic substrates is modest at best, and the process is thus likely to be kinetically hampered. Boranes provided an interesting exception to these trends. Unlike their other second row counterparts they had surprisingly high CCI values, comparable to that of EPHP, presumably due to the stabilizing effect of σ donation on the boron halide bond.

Achieving thermodynamic viability represents a necessary but not sufficient condition for a successful radical dehalogenation process. Thus, while CCI values are useful for ruling out thermodynamically unsuitable chain carriers, further analysis is required to confirm the kinetic suitability of the remaining candidates. Using dehalogenation of isopropyl bromide as a case study, we studied the kinetic performance of one of the better carbon-centered chain carriers, H−CH(OCH$_3$)CH$_3$, and two promising noncarbon-centered chain carriers, H−B(CH$_3$)$_2$ and H−BiH(O)O$^-$, comparing the results with corresponding calculated results for EPHP and with literature data for H−SnBu$_3$ and H−SiTMS$_3$. It was found that the rate-determining propagation step for successful chain carriers had rate coefficients of at least 10^4 L mol^{-1} s^{-1} (in the case of EPHP) and values of up to 10^6 L mol^{-1} s^{-1} in the case of the best-performing reagent, H−SnBu$_3$. As might have been anticipated from its low CCI value, for H−CH(OCH$_3$)CH$_3$, the rate coefficients for *both* propagation steps fall well below those of the rate-determining propagation step in successful processes and there seems little scope for further optimization of such carbon-based species. The two novel noncarbon-centered chain carriers tested, H−B(CH$_3$)$_2$ and H−BiH(O)O$^-$, also failed on kinetic grounds, each having a rate coefficient for its rate-limiting propagation steps (hydrogen donation for H−B(CH$_3$)$_2$ and halogen abstraction for H−BiH(O)O$^-$) that was well below those of successful chain carriers. However, in line with their high CCI values, their non-rate-determining propagation step was several orders of magnitude faster than required for a successful process, and this provides a large cushion that can be exploited when optimizing the rate of the slower reaction through substitution changes. Indeed success in this direction has already been achieved for the borane-based reagents,[36] and both classes of compounds would be worth further investigation as tin-free radical reducing agents.

ASSOCIATED CONTENT

Supporting Information. Further computational results including chain carrier indices of all species under all studied reaction conditions, and complete optimized geometries in the form of Gaussian archive entries and corresponding total free energies for all studied species. This material is available free of charge via the Internet at http://pubs.acs.org.

AUTHOR INFORMATION

Corresponding Author

*mcoote@rsc.anu.edu.au

Present Addresses

[†]National University of Singapore, 3 Science Drive, Singapore 117543

ACKNOWLEDGMENT

We gratefully acknowledge financial support from the Australian Research Council under their Centres of Excellence program and the generous allocation of computing time on the National Facility

of the National Computational Infrastructure. We also thank Associate Professor Michael Sherburn and the late Professor Athel Beckwith for many useful discussions.

REFERENCES

(1) For a recent review see: Rowlands, G. J. *Tetrahedron* **2009**, *65*, 8603–8655.
(2) Almetti, J. A.; Hamanaka, E. S.; Johnson, D. A.; Kellogg, M. S. *Tetrahedron Lett.* **1979**, *20*, 4631–4634.
(3) Wutts, P. G. M.; D'Costa, R.; Butler, W. *J. Org. Chem.* **1984**, *49*, 2582–2588.
(4) Minin, P. L.; Walton, J. C. *J. Org. Chem.* **2003**, *68*, 2960–2963.
(5) (a) Ingham, R. K.; Rosenberg, S. D.; Gilman, H. *Chem. Rev.* **1960**, *60*, 459–539. (b) Boyer, I. J. *Toxicology* **1989**, *55*, 253–298.
(6) (a) Chatgilialoglu, C.; Griller, D.; Lesage, M. *J. Org. Chem.* **1988**, *53*, 3641–3642. (b) Chatgilialoglu, C.;Ferreri, C.; Gimisis, T. In *The Chemistry of Organic Silicon Compounds*; Rappoport, Z., Apeloig, Y., Eds.; John Wiley & Sons: Chichester, UK, 1998; Vol. 2, Part 2, pp 1539−1579. (c) Chatgilialoglu, C. In *The Chemistry of Organic Silicon Compounds*; Rappoport, Z., Apeloig, Y., Eds.; John Wiley & Sons: Chichester, UK, 2001; Vol. 3, pp 341−390. (d) Chatgilialoglu, C. In *Radicals in Organic Synthiesis*; Renaud, P., Sibi, M. P., Eds.; Wiley-VCH: Weinheim, Germany, 2001; Vol. 1, pp 28−49.
(7) (a) Barton, D. H. R.; Jang, D. O.; Jaszberenyi, J. C. *Tetrahedron Lett.* **1992**, *33*, 5709–5712. (b) Barton, D. H. R.; Jang, D. O.; Jaszberenyi, J. C. *J. Org. Chem.* **1993**, *58*, 6838–6842.
(8) Perchyonok, V. T. *Tetrahedron Lett.* **2006**, *47*, 5163–5165.
(9) Longshaw, A. I.; Carland, M. W.; Krenske, E. H.; Coote, M. L.; Sherburn, M. S. *Tetrahedron Lett.* **2007**, *48*, 5585–5588.
(10) As noted by a reviewer, this good correlation between the CCI and ΔBDFE values implies that in principle, any R−X BDFE can be calculated from knowledge of the corresponding R−H BDFE (a derivation of this result is provided in Appendix S2 of the Supporting Information). However, in practice, the scatter in the CCI versus ΔBDFE relationship is magnified when it is used to calculate individual BDFE values, and the resulting errors are too large to be synthetically useful.
(11) Hehre, W. J.; Radom, L.; Schleyer, P. v. R.; Pople, J. A. *Ab Initio Molecular Orbital Theory*; Wiley: New York, 1986.
(12) Koch, W.; Holthausen, M. C. *A Chemist's Guide to Density Functional Theory*; Wiley-VCH: Weinheim, Germany, 2000.
(13) Frisch, M. J., et al. *Gaussian 03*, Revision B.03; Gaussian, Inc.: Pittsburgh, PA, 2003.
(14) *MOLPRO*, version 2006.1, a package of *ab initio* programs; Werner, H.-J., Knowles, P. J., Lindh, R., Manby, F. R., Schütz, M., and others, see http://www.molpro.net
(15) Izgorodina, E. I.; Brittain, D. R. B.; Hodgson, J. L.; Krenske, E. H.; Lin, C. Y.; Namazian, M.; Coote, M. L. *J. Phys. Chem. A* **2007**, *111*, 10754–10768.
(16) Scott, A. P.; Radom, L. *J. Phys. Chem.* **1996**, *100*, 16502–16513.
(17) Rassolov, V. A.; Ratner, M. A.; Pople, J. A.; Redfern, P. C.; Curtiss, L. A. *J. Comput. Chem.* **2001**, *22*, 976–984.
(18) Hay, P. J.; Wadt, W. R. *J. Chem. Phys.* **1985**, *82*, 284–298.
(19) Henry, D. J.; Sullivan, M. B.; Radom, L. *J. Chem. Phys.* **2003**, *118*, 4849–4860.
(20) Peterson, K. A. *J. Chem. Phys.* **2003**, *119*, 11099–11112.
(21) Coote, M. L.; Lin, C. Y.; Beckwith, A. L. J.; Zavitsas, A. A. *Phys. Chem. Chem. Phys.* **2010**, *12*, 9597–9610.
(22) Vreven, T.; Morokuma, K. *J. Comput. Chem.* **2000**, *21*, 1419–1432.
(23) See for example: (a) Stull, D. R.; Westrum, E. F., Jr.; Sinke, G. C. *The Thermodynamics of Organic Compounds*; John Wiley & Sons: New York, 1969. (b) Robinson, P. J. *J. Chem. Educ.* **1978**, *55*, 509–510. (c) Steinfeld, J. I.; Francisco, J. S.; Hase, W. L. *Chemical Kinetics and Dynamics*; Prentice Hall: Englewood Cliffs, NJ, 1989.
(24) These are summarized in the Supporting Information of a previous publication: Coote, M. L.; Radom, L. *Macromolecules* **2004**, *37*, 590–596.
(25) Cossi, M.; Rega, N.; Scalmani, G.; Barone, V. *J. Comput. Chem.* **2003**, *24*, 669.
(26) Toh, J. S.-S.; Huang, D. M.; Lovell, P. A.; Gilbert, R. G. *Polymer* **2001**, *42*, 1915–1920.
(27) Merrick, J. P.; Moran, D.; Radom, L. *J. Phys. Chem. A* **2007**, *111*, 11683–11700.
(28) Eckart, C. *Phys. Rev.* **1930**, *35*, 1303–1309.
(29) For more details on this procedure, see for example: Coote, M. L.; Collins, M. A.; Radom, L. *Mol. Phys.* **2003**, *101*, 1329–1338.
(30) Luo, Y.-R. *Comprehensive Handbook of Chemical Bond Energies*; CRC Press: Boca Raton, FL, 2007.
(31) (a) Shaik, S.; Maitre, P.; Sini, G.; Hiberty, P. C. *J. Am. Chem. Soc.* **1992**, *114*, 7861–7866. (b) Lauvergnat, D.; Hiberty, P. C.; Danovich, D.; Shaik, S. *J. Phys. Chem.* **1996**, *100*, 5715–5720. (c) Shurki, A.; Hiberty, P. C.; Shaik, S. *J. Am. Chem. Soc.* **1999**, *121*, 822–834.
(32) See for example: Mohan, R. *Nat. Chem.* **2010**, *2*, 336.
(33) (a) Zavitsas, A. A. *J. Chem. Educ.* **2001**, *78*, 417–419. (b) Coote, M. L.; Pross, A.; Radom, L. *Org. Lett.* **2003**, *5*, 4689–4692.
(34) We thank an anonymous reviewer for drawing our attention to this result.
(35) See for example: (a) Chatgilialoglu, C. *Acc. Chem. Res.* **1992**, *25*, 188–194. (b) Chatgilialoglu, C.; Newcomb, M. *Adv. Organomet. Chem.* **1999**, *44*, 67–112. (c) Newcomb, M. Small-Radical Chemistry. In *Handbook of Radical Polymerization*; Matyjaszewski, K., Davis, T. P., Eds.; John Wiley & Sons, Inc.: Hoboken, NJ, 2003; p 77.
(36) See for example: (a) Ueng, S.-H.; Fensterbank, L.; Lacôte, E.; Malacria, M.; Curran, D. P. *Org. Lett.* **2010**, *12*, 3002–3005. (b) Ueng, S.-H.; Brahmi, M. M.; Derat, E.; Fensterbank, L.; Lacôte, E.; Malacria, M.; Curran, D. P. *J. Am. Chem. Soc.* **2008**, *130*, 10082–10083.